氏　　名	MAI THI KIEU LIEN
学位の種類	博士(マテリアルサイエンス)
学位記番号	博材第 383 号
学位授与年月日	平成 27 年 9 月 24 日
論文題目	Study on Material Properties of Si Thin Films Crystallized on Yttria-Stabilized Zirconia in Solid Phase by Pulsed Laser Annealing （パルスレーザアニールによりイットリア安定化ジルコニア上に固相結晶化した Si 薄膜の膜質に関する研究）
論文審査委員	主査　堀田　將　北陸先端科学技術大学院大学　准教授 下田　達也　同　教授 徳光　永輔　同　教授 大平　圭介　同　准教授 東　清一郎　広島大学　教授

Study on Material Properties of Si Thin Films Crystallized on Yttria-Stabilized Zirconia in Solid Phase by Pulsed Laser Annealing

Horita Laboratory

Student number: 1240206

Student name: Mai Lien Thi Kieu

1. Introduction:

In thin-film transistor (TFT) fabrication, although oxide and organic materials have been studied extensively for active channel material, the most prolonged and widely used materials are hydrogenated-amorphous silicon (a-Si:H) and polycrystalline silicon (poly-Si). The a-Si:H TFT can be fabricated at a lower cost than poly-Si TFT. However, low carrier mobility (~ 1 $cm^2V^{-1}s^{-1}$), instability, and low reliability are its drawbacks, which can be addressed by poly-Si TFT. As a fabrication method, generally, crystallization of deposited a-Si films has been widely used to obtain high quality films. It can be carried out by several techniques, such as solid phase crystallization (SPC), metal-induced crystallization (MIC), metal-induced lateral crystallization (MILC), and pulsed laser annealing (PLA). Among them, although PLA has become a leading technique to fabricate poly-Si films at low temperature, high surface roughness and non-uniform-sized grain in the melted poly-Si films limit the extent of applications. To overcome these limitations, we proposed using a crystallization-induction (CI) layer of yttria-stabilized zirconia [$(ZrO_2)_{1-x}(Y_2O_3)_x$:YSZ] combined with PLA for micro-crystallization with non-intentional melting. In this method, an amorphous Si (a-Si) film is deposited on a YSZ layer that covers the surface of a glass substrate. Then, the a-Si film is crystallized in solid phase by the PLA method at room temperature. Since YSZ has a small lattice mismatch of ~5% and the same cubic crystal structure as Si, it can be expected that the obtained poly-Si film will have uniform grain size and crystallographic information, owing to the crystallographic information of the YSZ layer. The combination of the CI layer and SPC-PLA methods is thought to have high potential not only for eliminating the drawback of the melting-PLA method, but also for satisfying the demands for the application of poly-Si TFTs.

The main research purpose is to improve crystallization technique of Si thin film by using YSZ-CI layer combined with SPC-PLA methods. In order to achieve the purpose, firstly, we investigate the crystallinity of pulsed-laser crystallized Si films on YSZ layers, comparing with those on glass substrates. From the obtained results, for further improving the crystallinity of Si films, we propose a new two-step irradiation method using a pulsed laser, which will be mentioned later in more details. We then investigate crystalline quality and electrical properties of crystallized Si films with/without the YSZ layers obtained by the new method, in comparison with the conventional method.

2. Experimental:

A 60 nm YSZ (111)-CI layer is deposited on a cleaned quartz substrate at a substrate temperature of 50 °C by reactive magnetron sputtering. Then, a 60 nm a-Si film is deposited on a YSZ/quartz substrate by e-beam evaporation at 300 °C. For comparison, an a-Si film is also deposited directly on a quartz substrate without a YSZ layer. For investigating electrical properties, undoped and P-doped samples are prepared. P ion implantation is performed at an acceleration voltage of 40~50 kV and the average estimated doping concentration in the Si film is about 3.7×10^{17}~4.9×10^{19} cm^{-3}. Then, crystallization of the a-Si films in solid phase is carried out by PLA together with activation of the implanted P ions in N_2 ambient. For this annealing, we use the new two-step method, which is illustrated in Fig. 1(b), in comparison with the conventional or one-step method in Fig. 1(a). The pulsed laser is Nd:YAG laser (λ = 532 nm) with a repetition frequency of 10 Hz and a pulsed duration of 6~7 ns. In the two-step method, firstly, a-Si films are irradiated at a low initial energy density E_i to generate nuclei, following by irradiation at a high growth energy density E_g to accelerate the nuclei growth and film crystallization without random nucleation in the bulk. For comparison, some samples without doping are also prepared by a conventional method at a fixed high energy density E.

The crystallization degree of Si films without doping is estimated by two kinds of Raman spectroscopies. For evaluation of average crystalline quality of a whole Si film, we used He-Ne laser with the excitation wavelength of 633 nm as a probe beam. The

absorption depth D for a-Si is more than 200 nm. For local evaluation of the surface or interface with YSZ of the Si film, we used He-Cd laser with the wavelength of 442 nm. The Ds for a-Si and poly-Si are 20–30 nm and more than 200 nm, respectively. The crystalline fraction X_c is determined by $X_c = (I_c + I_m) = (I_c + I_m + I_a)$, where I_c, I_m, and I_a are integrated intensities of crystalline silicon (c-Si), intermediate-crystalline silicon (m-Si), and a-Si peaks, respectively. The grain size of poly-Si films after Secco etching is observed by scanning electron microscopy (SEM). The cross-section of the Si films on the YSZ/glass substrate without doping was observed by transmission electron microscopy (TEM). The surface crystallinity of Si films with/without the YSZ layer is observed by reflection high-energy electron diffraction (RHEED) after crystallization. The average carrier concentration n, Hall mobility μ_H, and conductivity σ over in-grains and grain boundaries of the crystallized Si films are measured by AC Hall effect and conductivity measurements, using the Van der Pauw method at a magnetic field of 0.4 T. The measurement temperature is varied from room temperature (RT) to 300 °C, and activation energies of n, μ_H, and σ are estimated.

3. Results and discussion:

Figure 2(a) shows the dependence of crystalline fraction X_c on pulse number N using a He-Ne laser beam for Raman spectroscopy, where the irradiation energy density is a parameter. The Si films in this figure were crystallized by the conventional method. It can be seen that increasing N (or annealing time) makes X_c of Si films increase. At the lower energy density E, X_c is smaller. At the higher E, X_c increases rapidly. The both X_c's become saturated even a the small N. X_c's of Si films on glass substrates are found to be higher, or faster crystallization, than those on YSZ layers at the same E and N. This is because optical absorption in Si film for Si/glass is larger than that for Si/YSZ/glass. The difference in optical absorption between them is calculated to about 10 %, taking multi-reflection into account. Figure 2(b) shows the He-Cd Raman spectra from front and back side measurements of the Si/YSZ/glass, where annealing conditions of E and N are 78 – 80 mJ/cm^2 and 10, respectively, near the onset of X_c saturation as enclosed by a solid circle in Fig. 2(a). Although, from the front side measurement, a very small c-Si peak might be observed, from the back side measurement, a relative high and sharp c-Si peak is clearly seen as shown by dashed circles in Fig. 2(b). This indicates enhanced crystallization growth from the interface between Si and YSZ layers and few nucleation near the surface of Si film. From this result, it can be inferred that annealing at lower E can promote the interface crystallization to keep relatively good quality. However, with only lower E, complete crystallization is impossible.

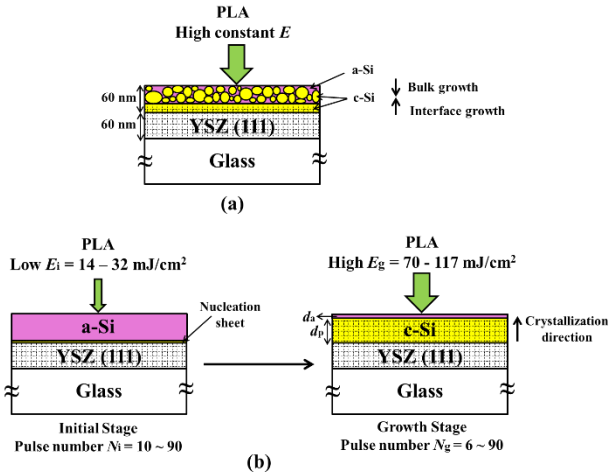

Fig. 1 Schematic illustrations of crystallization in Si/YSZ/glass for the (a) conventional or one-step and (b) new two-step methods together with the irradiation conditions.

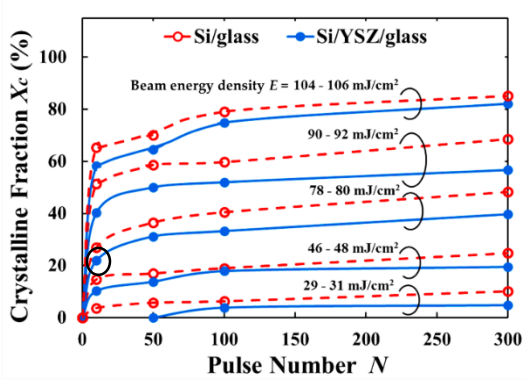

(a) Dependence of crystalline fraction X_c on pulse number N by He-Ne system with absorption depth D (a-Si) > 200 nm.

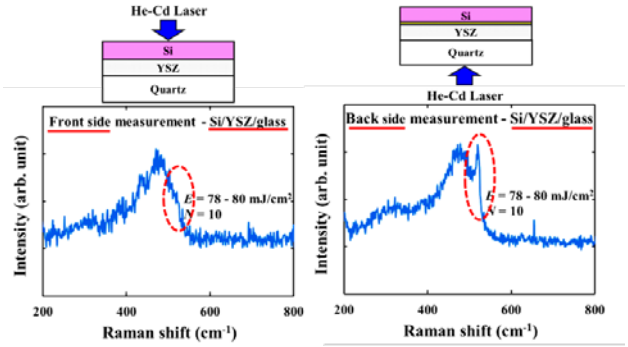

(b) Raman spectra of the Si/YSZ/glass by He-Cd system with D (a-Si) = 20 ~ 30 nm and D (c-Si) > 200 nm.

Fig. 2 Raman analysis results.

From the above results and discussion, in order to obtain a fully crystallized Si film with high quality, we tried to crystallize them with the two-step method as shown in Fig. 1(b). The initial irradiation at a low energy E_i and small N_i makes nuclei at the

interface without in-bulk, and the growth irradiation at high energy E_g and larger N_g enhances crystallization growth from the interface nuclei to the surface with high rate, which should be faster than bulk crystallization. Table I shows the comparison of the typical X_c and FWHM values of the c-Si peak of Si/glass and Si/YSZ/glass for the conventional method with N = 100 and the two-step method with N_i = 10 and N_g = 90, which are obtained by He–Ne Raman spectral analysis. For the conventional method, the samples were irradiated at a high constant E. In the two-step method, two irradiation conditions (A) and (B) were used, shown in Table I. Both the optimized E_i and E_g for Si/YSZ/glass are slightly higher than those for Si/glass due to a small optical absorption difference between them as mentioned before. Firstly, it can be clearly seen that the crystalline quality of the crystallized Si films is more improved by the two-step method (labelled ③ and ④) for both the Si/glass and Si/YSZ/glass structures than by the conventional method (labelled ① and ②). That is, a higher X_c and a smaller FWHM are obtained by the two-step method despite using the same total pulse number and a lower total irradiation energy density E_t, where $E_t = E \cdot N$ for the conventional method and $E_t = E_i \cdot N_i + E_g \cdot N_g$ for the two-step method. Next, we compare the Si/YSZ/glass case ④ with the Si/glass case ③ in the two-step method. Although X_c = 82% for Si/YSZ/glass is apparently smaller than 87% for Si/glass, the FWHM for both is approximately 6.0. This indicates that it is still possible to increase X_c and improve crystalline quality for Si/YSZ/glass by optimizing E. Actually, using the optimized irradiation condition for Si/YSZ/glass in the two-step method, we obtain a higher X_c and a smaller FWHM in ⑤ than in ③ and ④. From these results, it can be concluded that a Si film with a higher crystalline quality can be obtained on YSZ/glass than on the glass substrate for both the conventional and two-step methods, which may be due to the CI effect of the YSZ layer.

Table I. X_c and FWHM of c-Si peaks of Si/glass and Si/YSZ/glass for the conventional and two-step methods.

Method		Irradiation conditions	Si/glass	Si/YSZ/glass
Conventional		E = 104 – 106 mJ/cm², N = 100	X_c = 79% ① FWHM = 8.1	X_c = 75% ② FWHM = 7.6
Two-step	(A)	E_i = 18 – 22 mJ/cm², N_i = 10 E_g = 106 – 109 mJ/cm², N_g = 90 (optimized for Si/glass)	X_c = 87% ③ FWHM = 6.0	X_c = 82% ④ FWHM = 6.1
	(B)	E_i = 20 – 24 mJ/cm², N_i = 10 E_g = 111 – 114 mJ/cm², N_g = 90 (optimized for Si/YSZ/glass)	/	X_c = 91% ⑤ FWHM = 5.2

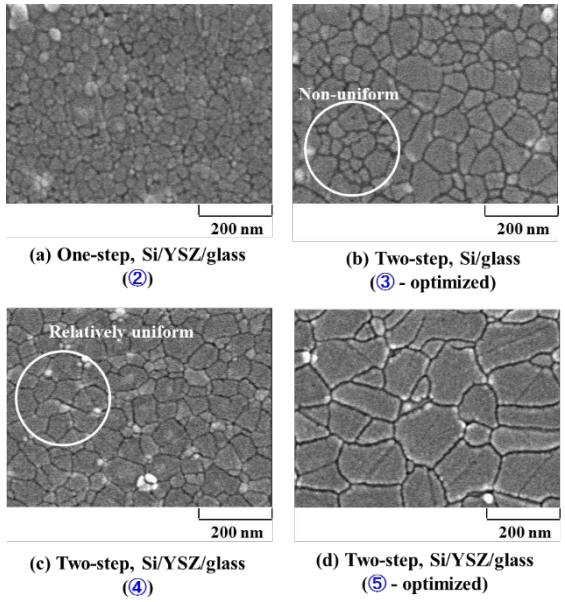

(a) One-step, Si/YSZ/glass (②)
(b) Two-step, Si/glass (③ - optimized)
(c) Two-step, Si/YSZ/glass (④)
(d) Two-step, Si/YSZ/glass (⑤ - optimized)

Fig. 3 SEM images of the Secco-etched Si films crystallized by the conventional and two-step methods. (a)–(d) irradiation conditions are the same as those indicated by ②-⑤ in Table I, respectively.

To determine the effect of the two-step method clearly, by SEM, we observed Secco-etched Si films crystallized by both the conventional and two-step methods. The irradiation conditions are the same as those in Table I. Figure 3(a) shows the SEM image of the Si film irradiated by the conventional method while Figs. 3(b)–3(d) show those by the two-step method, where the sample structures are Si/YSZ/glass except for (b), i.e., Si/glass. The labels ②-⑤ in Fig. 3 correspond to the numbers or the same irradiation conditions in Table I. Firstly, from the comparison between Fig. 3(a) and Fig. 3(c), it can be seen that large grains are obtained in Si/YSZ/glass by the two-step method. This clearly indicates the effectiveness of the two-step method in promoting the crystallization of the a-Si film. Next, we compare the Si film on glass with that on YSZ in the two-step method under the same irradiation conditions, as shown in Figs. 3(b) and 3(c), respectively. It can be found easily that the difference in grain size or grain size non-uniformity is larger in the Si/glass than in the Si/YSZ/glass, for instance, as shown by circles in Figs. 3(b) and 3(c). For Si/YSZ/glass irradiated under its optimized conditions as shown in Fig. 3(d), the grain size apparently becomes larger than that for Si/glass under its optimized irradiation conditions [Fig. 3(b)]. This result indicates better quality of the Si film on the YSZ layer than on the glass substrate, even by using the two-step method.

Figures 4 and 5 show the Arrhenius plots of conductivity σ with respect to the reciprocal of the measurement temperature T for the crystallized undoped and P-doped Si/YSZ/glass and Si/glass structures, respectively, with different doping concentrations. The Si films in these structures were crystallized by the two-step method. The activation energies $E_{\sigma i}$ for σ are also shown in these figures, where i = 1 to 5. It was found that all of Si films are n-type. On the whole, excepting at high doping concentration of 4.9×10^{19} cm^{-3}, the conductivity exhibits the behavior of an activation process for both the undoped and P-doped films on both Si/YSZ/glass and Si/glass structures. For the films at the highest doping concentration of 4.9×10^{19} cm^{-3}, the saturation tendency of conductivity can be

attributed mainly to the saturation of carrier concentration. In Fig. 4, the activation energy of the undoped Si/YSZ/glass film is changed from 0.25 to 0.55 eV around 100 ºC. Since $E_{\sigma 2}$ is near half of energy gap $E_g/2$ or intrinsic energy level E_i, the carrier may be generated from carrier traps at grain boundaries due to thermal excitation. On the other hand, in the low temperature region (T ≤ 100 ºC), carriers are excited from the some donors with an impurity level around 0.46 eV (data are not shown). Also, at the low temperature, free carriers are hardly excited from the trap levels at the grain boundaries. For the doped Si/YSZ/glass cases, the activation energies are lower than $E_{\sigma 2}$ = 0.55 eV of the undoped film and decrease with increasing doping concentration. This is probably because doped P ions segregate mainly into grain boundaries and passivate electrical defects. The amount of passivated defects increases with doping concentration, as a result, the conductivity increases. However, at higher doping concentration, the amount of dopant for passivation is enough and some doped P atoms are thermally activated from the normal donor level of 0.044 eV. For example, for the doping concentration of 4.9×10^{19} cm^{-3}, almost dopant P atoms give free electron carriers at RT. Therefore, E_σ is lower value of 0.01 eV (Si/YSZ/glass) or 0.03 eV (Si/glass).

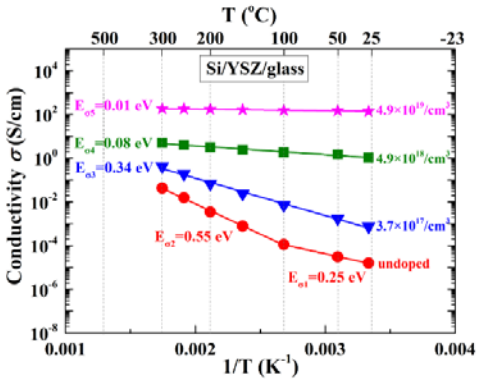

Fig. 4 Measurement temperature dependences of conductivity σ for the undoped and doped Si/YSZ/glass structures crystallized by the two-step method.

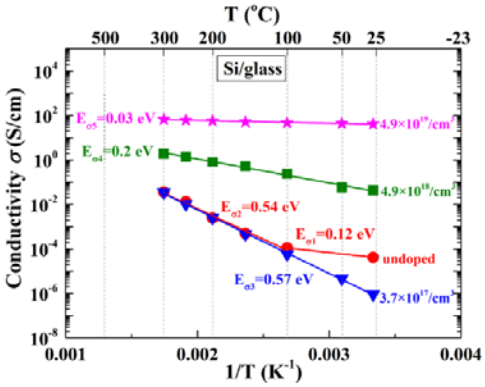

Fig. 5 Measurement temperature dependences of conductivity σ for the undoped and doped Si/glass structures crystallized by the two-step method.

In Fig. 5 of the Si/glass films, the conductivities are almost the same for both the undoped and low P-doped (3.7×10^{17} cm^{-3}), which means that the P-doping is not effective. Although the obtained Hall mobility for the low P-doped film is a little higher than that of the undoped one, the carrier concentrations (e.g., ~1.5×10^{14} cm^{-3} at 100 ºC) are nearly the same for both cases (the data are not shown). This is probably because the amount of the P dopant atoms are not so much to passivate most of the defects in the Si/glass film, compared with the Si/YSZ/glass one. The higher defect density in the Si/glass than in the Si/YSZ/glass also leads to the lower conductivity and higher activation energy in the former than in the latter at the same doping concentration. From the above results, it can be concluded that electrical property of the Si films on YSZ layers are much better than those on the glass substrates.

Figures 6(a) and (b) show typical transfer characteristics of the fabricated TFTs for the **Si/YSZ/glass** and **Si/glass** structures with $W = L$ = 40 μm. It can be seen that the TFTs can operate with relatively small off leakage current of ~10^{-12} A. The field-effect mobility for TFTs fabricated on the **Si/YSZ/glass** is about twice higher than that on the **Si/glass**. We estimated and summarized several important parameters of the device characteristics for the two structures of the Si/glass and Si/YSZ/glass. The field-effect mobility (μ_{eff}) and subthreshold swing (S.S) are evaluated from the linear and subthreshold regions, respectively, at V_D = 0.1 V. The ON/OFF current ratio is defined as the ratio of maximum drain current I_{Dmax} over minimum drain current I_{Dmin} within the measured range of I_D-V_G curve at V_D = 0.1 V. The threshold voltage (V_{th}) is determined by an interception of linear extrapolation of the I_D-V_G curve at V_D = 0.1 V. Table I summarizes the average values of device parameters together with their standard deviations of the TFTs with $W = L$ = 40 μm for the two structures. For each structure, 15 TFTs were measured. It can be seen that the TFTs fabricated on the **Si/YSZ/glass** structure exhibit a relatively higher μ_{eff} with smaller deviation than those on the Si/glass. The average V_{th} and average S.S of TFTs fabricated on the **Si/YSZ/glass** are both smaller with smaller deviations than those on the **Si/glass**. On the other hand, the average ON/OFF current ratio of TFTs fabricated on the Si/YSZ/glass is a little lower than those on the Si/glass. The field-effect mobility, threshold voltage, and subthreshold swing are strongly affected by the presence of grain boundaries and defects inside the channel. Therefore, comparing to the TFTs fabricated on the Si/glass, the relatively better performance of the TFTs fabricated on the Si/YSZ/glass are considered owing to the better crystalline quality of the Si film on the YSZ/glass. This is thank to the CI effect of the YSZ layer as discussed in the previously. The superior device-to-device uniformity in performance (expressed

by smaller standard deviations) of the TFTs fabricated on the **Si/YSZ/glass** than on the **Si/glass** is considered to be due to the more uniform grain size and crystalline defects distributions in the Si films for the former than for the latter.

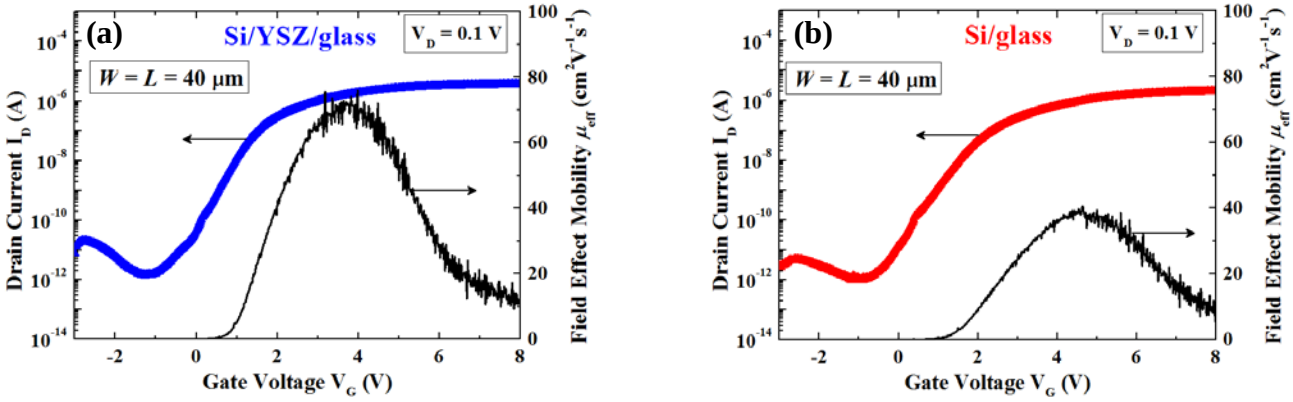

Fig. 6 Transfer characteristics of fabricated poly-Si TFTs for (a) the Si/YSZ/glass and (b) Si/glass structures with W=L=40 μm.

Table I Average values of μ_{eff}, V_{th}, and S.S together with their standard deviations, and average ON/OFF ratio of the TFTs with W = L = 40 μm for the two structures of the Si/glass and Si/YSZ/glass.

	Field-effect mobility μ_{eff} ($cm^2V^{-1}s^{-1}$)		Threshold voltage V_{th} (V)		Subthreshold swing S.S (mV/dec.)		ON/OFF ratio
	Average value	Standard deviation	Average value	Standard deviation	Average value	Standard deviation	Average value
Si/glass	40.3	28	2.83	0.78	426	99	1.74×10^6
Si/YSZ/glass	78.1	18	2	0.22	306	31	9.14×10^5

4. Conclusion:

We crystallized Si films on glass substrates with/without a YSZ-CI layer in the solid phase by PLA, and investigated not only their crystalline but also electrical properties. It was found that, for Si/YSZ/glass, nucleation occurs faster at the YSZ interface than in the bulk of the a-Si film at a low energy density E. For further improving the crystallinity of the Si films, we proposed the two-step method. The Raman analysis and SEM observation show that higher crystallization degree with better quality, and large-sized grains were obtained by the two-step method compared with the conventional method at the same total pulse number N and high total irradiation energy density E_t. Comparing the Si/YSZ/glass and Si/glass at their own optimized irradiation conditions, we obtained a higher crystallization degree with better quality in the former. The electrical property measurement results for both the undoped and doped Si films revealed that higher carrier concentration, Hall mobility, and conductivity are obtained for the Si/YSZ/glass structure compared with those of the Si/glass. Further, we fabricated poly-Si TFTs on both the structures. The device parameters of μ_{eff}, V_{th}, S.S, and ON/OFF current ratio of the fabricated TFTs were estimated as well as their uniformity. It was found that the TFTs fabricated on the Si/YSZ/glass exhibit a relatively better performance and superior device-to-device uniformity than those on the Si/glass. This result is considered owing to the better crystalline quality of the Si film on the YSZ/glass and uniform distribution of grains as well as crystalline defects, which indicating effectiveness of the crystallization-induction effect of the YSZ layer.

References: 1) M. T. K. Lien and S. Horita, Jpn. J. Appl. Phys. **53**, 03CB01 (2014) and refs. in there.

2) M. T. K. Lien and S. Horita, Jpn. J. Appl. Phys. **54**, 03CA01 (2015) and refs. in there.

Keywords: poly-Si, pulsed laser, YSZ, crystallization-induction layer, low temperature, solid phase crystallization, TFT.

論文審査の結果の要旨

耐熱性の低い安価なガラス基板上に低温形成した薄膜トランジスタ(TFT)は、薄型テレビなどの電子機器に用いられるが、さらなる低コスト、高性能化のために様々な半導体材料が検討されている。その中でも、高移動度、経時的安定性などの観点から多結晶 Si が注目されている。しかし、多結晶 Si 薄膜の主要作製法である溶融結晶化法では、結晶核がランダムに発生・成長するために、膜中の結晶粒径・欠陥分布もランダムとなり、個々のデバイス特性の均一性が悪く、機器高性能化の障害となっている。

これに対して本研究室では、結晶性絶縁体イットリア安定化ジルコニア(YSZ)層をガラス基板上に堆積し、YSZ の結晶情報によりその上に形成する多結晶 Si 薄膜の特性の均一化を図っている。しかし、粒径などの均一性は上がるものの、400℃以上の高い形成温度、無視できない膜表面荒れ、YSZ 層からの不純物拡散などの問題がある。そこで本論文では、多結晶化 Si 薄膜の形成に、YSZ 層上に堆積した非晶質 Si(a-Si)薄膜をパルスレーザアニール(PLA)により固相結晶化する方法を提案し、上記問題の解決を図り、最終的には TFT の作製とその特性評価で実証を試みている。

まず、YSZ 層の結晶情報伝達効果を明らかにするために、PLA のパルス数 N、照射エネルギーE を変化させて、結晶化膜の作製と評価を YSZ 層の無いものと比較して行っている。その結果、結晶化膜の結晶性の N,E 依存性を明らかにすると共に、YSZ 層が結晶性の向上、均一化に有効であることを示している。

次に、上記基礎データを基に、結晶粒径の拡大と結晶欠陥密度の低減を図るために、2 step 照射法を提案・検討している。本手法は、a-Si 薄膜中でのランダム核発生を抑制し、YSZ/Si 界面にだけ結晶核を発生させるために、はじめに低 E によるレーザ照射を行い、次にその結晶核からの成長を膜表面まで素早くさせるために、高 E による照射を行うものである。その結果、2 step 法により粒径が従来法の 20nm から 200nm 近くに増加し、結晶性も明らかに向上した。さらに、膜表面荒れは溶融結晶化法に比べて、1/10 以下となり、Zr、Y の不純物拡散も高温堆積時に比べて２桁ほど低減できることを明らかにした。

続いて、上記 2 step 法による結晶化膜の電気的特性を見るために、抵抗率及び交流ホール効果測定を、不純物 P 濃度を変化させて行った。この時、YSZ 層有無の比較を同時に行い、YSZ 層の効果も見た。その結果、YSZ 層のあるものが、導電率がより高く、結晶欠陥による電気的影響がより低い P 濃度で低減することを見出し、YSZ 層による効果の優位性を電気的にも明らかにした。

最後に、YSZ 層有る、無しの両試料上に 2 step 法により形成した多結晶 Si 薄膜を用いて TFT を作製し、その特性を比較・検討した。その結果により、YSZ 層の有無で平均電界効果移動度がそれぞれ約 80、40 cm^2/Vs、またその標準偏差が 18, 28 cm^2/Vs となり、前者の方が優れた特性、分布であること示した。同様なことは、閾値電圧、subthreshold swing に

も見られ、YSZ 層を用いた方が用い無いものよりも、デバイス特性とともにその均一性も向上することを明らかにした。

以上、本論文は、従来問題となっている低温多結晶 Si 薄膜の膜質の不均一性を YSZ 層と PLA による 2 step 法を用いることにより大幅に解決できることを、膜構造ばかりでなく、作製した TFT 特性からも実証したものであり、これらの知見は、学術的に貢献するところが大きい。よって博士（マテリアルサイエンス）の学位論文として十分価値あるものと認めた。